



African biomass burning is a substantial source of phosphorus deposition to the Amazon, Tropical Atlantic Ocean, and Southern Ocean

Anne E. Barkley^a, Joseph M. Prospero^a, Natalie Mahowald^b, Douglas S. Hamilton^b, Kimberly J. Popendorf^a, Amanda M. Oehlert^a, Ali Pourmand^a, Alexandre Gatineau^c, Kathy Panechou-Pulcherie^c, Patricia Blackwelder^{a,d}, and Cassandra J. Gaston^{a,1}

^aRosenstiel School of Marine and Atmospheric Sciences, University of Miami, Miami, FL 33149; ^bDepartment of Earth and Atmospheric Sciences, Cornell University, Ithaca, NY 14853; ^cATMO Guyane, 97343 Remire-Montjoly, Guyane (French Guiana), France; and ^dCenter for Advanced Microscopy, Department of Chemistry, University of Miami, Coral Gables, FL 33146

Edited by John H. Seinfeld, California Institute of Technology, Pasadena, CA, and approved June 28, 2019 (received for review April 9, 2019)

The deposition of phosphorus (P) from African dust is believed to play an important role in bolstering primary productivity in the Amazon Basin and Tropical Atlantic Ocean (TAO), leading to sequestration of carbon dioxide. However, there are few measurements of African dust in South America that can robustly test this hypothesis and even fewer measurements of soluble P, which is readily available for stimulating primary production in the ocean. To test this hypothesis, we measured total and soluble P in long-range transported aerosols collected in Cayenne, French Guiana, a TAO coastal site located at the northeastern edge of the Amazon. Our measurements confirm that in boreal spring when African dust transport is greatest, dust supplies the majority of P, of which 5% is soluble. In boreal fall, when dust transport is at an annual minimum, we measured unexpectedly high concentrations of soluble P, which we show is associated with the transport of biomass burning (BB) from southern Africa. Integrating our results into a chemical transport model, we show that African BB supplies up to half of the P deposited annually to the Amazon from transported African aerosol. This observational study links P-rich BB aerosols from Africa to enhanced P deposition in the Amazon. Contrary to current thought, we also show that African BB is a more important source of soluble P than dust to the TAO and oceans in the Southern Hemisphere and may be more important for marine productivity, particularly in boreal summer and fall.

soluble and could be a more important source of SP transported to the TAO (15, 18, 23–25). Due to the buoyancy of smoke plumes, BB aerosols can be emitted directly into the free troposphere and the particles are typically smaller in size than dust increasing the atmospheric lifetime of BB during transport (26, 27).

The source and solubility of P that impacts the Amazon and TAO changes due to the seasonal migration of the Intertropical Convergence Zone (ITCZ) and seasonality of BB in Africa (28, 29). During the boreal winter and spring (December to April), African dust is the main aerosol transported to these ecosystems when the ITCZ is largely south of the equator (1, 5, 8, 12, 15). BB from the Sahel south of the Sahara can be cotransported with dust (3, 28, 30, 31) and potentially provides additional P to the Amazon and TAO in boreal winter and spring. During the boreal fall (September to November), the ITCZ is located at ~5° to 10°N, inhibiting African dust transport to South America (5, 32). There are few measurements of P over the TAO, but the measurements that exist suggest that both total P (TP) and SP can be elevated in fall (22, 33). BB from southern Africa has been speculated to reach South America and the TAO during this season (28, 34–36); however, the ability of African BB to supply TP and SP to the Amazon and the TAO has not been investigated.

dust | biomass burning | phosphorus | Atlantic Ocean | Amazon Basin

Deposition of phosphorus (P) by aerosols to P-depleted ecosystems modulates primary productivity and can consequently impact atmospheric carbon dioxide levels on a global scale (1–4). Every year, African dust is transported across the Tropical Atlantic Ocean (TAO) to South America in boreal winter and spring (5, 6). Nutrients associated with dust are hypothesized to alleviate P limitations (1, 7–10) on a timescale of days in marine environments to millions of years in tropical terrestrial ecosystems (4, 9, 11). P deposition to the Amazon from African dust has been estimated using remote sensing and models (8, 12, 13); however, P deposition associated with the long-range transport of nondust aerosol has not been measured.

The chemical composition of aerosols affects the solubility of P, which determines its bioavailability and how readily P is utilized by primary producers. In the ocean, soluble P (SP) is rapidly used and removed by marine organisms (14). In terrestrial environments, the residence time of P in soil is longer, facilitating the transformation of insoluble P into more bioavailable forms (9). African dust is thought to be the largest contributor of P to the Amazon and TAO (15), but its solubility is low (16–20). While P in dust can be transformed into more soluble forms via reactions with acids (20, 21), the importance of this process during transport is debated (19, 22, 23). In contrast, P in aerosols from biomass burning (BB) and fossil fuel combustion are more

Significance

Phosphorus (P) deposition from aerosols can stimulate primary productivity in P-depleted marine and terrestrial ecosystems. We tested the hypothesis that African dust fertilizes the Amazon Basin and Tropical Atlantic Ocean (TAO) by measuring wind-borne dust, P, and soluble P in samples collected at a coastal site on the northeastern edge of the Amazon. Using satellite data and models, we identified a previously underestimated source of soluble P: biomass burning aerosol transported from southern Africa that can supply P to the Amazon, TAO, and Southern Ocean. Because P associated with biomass burning emissions is more soluble than P in transported dust, biomass burning aerosols immediately impact P cycling and primary production, especially in marine ecosystems like the TAO.

Author contributions: A.E.B., J.M.P., K.J.P., and C.J.G. designed research; A.E.B. performed research; A.E.B., J.M.P., N.M., D.S.H., K.J.P., A.M.O., A.P., A.G., K.P.-P., P.B., and C.J.G. contributed new reagents/analytic tools; A.E.B., J.M.P., N.M., D.S.H., K.J.P., A.M.O., A.P., and C.J.G. analyzed data; and A.E.B., J.M.P., and C.J.G. wrote the paper.

The authors declare no conflict of interest.

This article is a PNAS Direct Submission.

Published under the PNAS license.

¹To whom correspondence may be addressed. Email: cgaston@rsmas.miami.edu.

This article contains supporting information online at www.pnas.org/lookup/suppl/doi:10.1073/pnas.1906091116/-DCSupplemental.

Published online July 29, 2019.

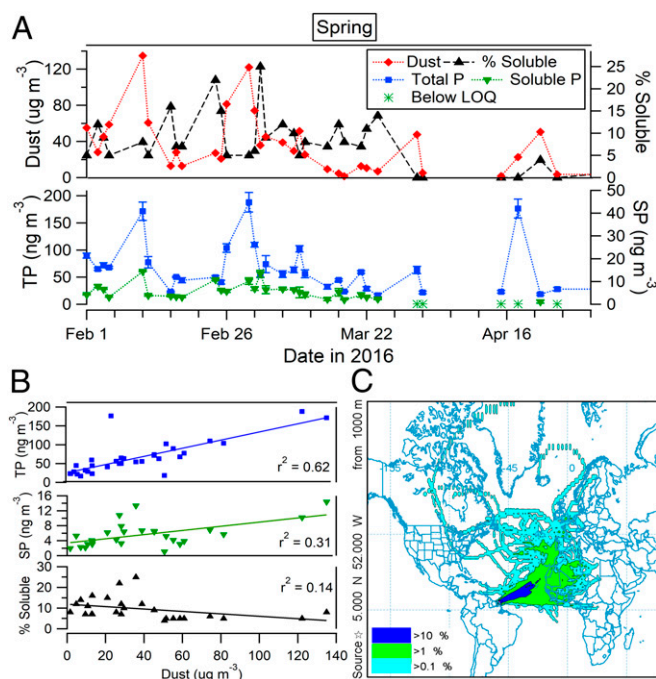


Fig. 1. Data are shown from spring only. *A* shows the dust concentration and percentage of SP in the *Top* and concentrations of TP and SP in the *Bottom*. Error bars for P measurements show one SD. *B* shows the correlation between dust and TP (*Top*), dust and SP (*Middle*), and percentage of soluble P and dust (*Bottom*). *C* shows HYSPLIT frequency plots of air mass back trajectories at 1,000 m initiated every 6 h from February 1 to March 31, 2016.

Here we present year-long measurements of P in aerosols transported to South America. Samples were collected in Cayenne, French Guiana (4.92°N, 52.31°W) at a site located on the northeastern part of the Amazon and coast of the TAO (*SI Appendix, Fig. S1*). We focus our analysis during boreal spring and fall 2016 to characterize the seasonal differences in the amount and solubility of P transported to Cayenne. A chemical transport model was used to estimate the contribution of African BB and dust to P deposition. Our results indicate that African BB is a significant source of P deposited to the Amazon and TAO, with further implications for oceans in the Southern Hemisphere.

Results

Contributions of P from African Dust to Cayenne in Spring. We first discuss P measurements during the spring (February to April) when African dust is at a maximum (5, 6). African dust measured at Cayenne in winter and spring is comparable in magnitude to dust measured in Barbados in summer (37). The daily average concentration of particulate matter with an aerodynamic diameter <10 μm (PM₁₀) is also highest in boreal winter and spring when it is correlated with dust ($r^2 = 0.86$; *SI Appendix, Fig. S2*), suggesting that dust dominates the aerosol burden in Cayenne in spring. To investigate the supply of P from dust, we compared the temporal variability of dust, total P, and SP concentrations as well as the percent of P that is soluble (Fig. 1*A*). The average TP concentration in spring was 66 ng m⁻³ and ranged from 17 to 188 ng m⁻³. TP was correlated with dust (Fig. 1*B, Top*), suggesting that dust is the main source of TP in spring. African soils contain up to 940 ppm of P (13, 16); however, we measured a higher average TP concentration of 1,080 ppm (*SI Appendix, Fig. S3A*). Using scanning electron microscopy (SEM), dust and BB were observed on filters collected in spring (*SI Appendix, Fig. S4*). Furthermore, the filter color of samples collected during spring was often gray-brown, indicating the presence of

dust and black carbon (BC) from BB (*SI Appendix, Fig. S5*). This evidence indicates that African BB was cotransported with dust, which is supported by previous studies (28, 30, 38) and is the likely aerosol source that increases TP in our samples above levels previously measured in Saharan soils. Air mass back trajectory (BT) analysis (Fig. 1*C*) confirms that air masses passed over the Sahara and the Sahel where BB is active, providing evidence that BB contributed to our observed TP.

Dust and SP were positively correlated (Fig. 1*B, Middle*); however, the percent of P that is soluble decreased with increasing dust (Fig. 1*B, Bottom*). We focus on quantifiable values of SP in Fig. 1*B* and show a similar correlation between dust and SP containing points below the limit of quantification (LOQ) in *SI Appendix, Fig. S3B*. For events when dust mass concentrations were >50 μg m⁻³, the average solubility of P in dust was just 5%. Atmospheric processing of dust could increase P solubility during transport (20, 21); however, changes in SP concentrations, which ranged from 2 to 14 ng m⁻³, were often out of phase with major dust events, suggesting that another source is a more important contributor of SP than dust. Because BB contains highly soluble P (22, 25, 39), the cotransport of BB to South America likely explains the uniform SP concentrations even on days with low dust.

In April 2016, we measured a marked decrease of SP, which is likely due to a decrease in the fire frequency in the Sahel (*SI Appendix, Fig. S6*) and is consistent with fire activity observed in other years (40, 41). This explains why little SP was measured despite high dust transport to Cayenne in April. This discordance further confirms the role of BB in supplying SP to South America in spring.

An Additional Supply of P from Southern African BB in Fall. Despite low dust mass concentrations, TP and SP concentrations were unexpectedly high in boreal fall. Fig. 2*A* shows low dust mass concentrations (e.g., 5–10 μg m⁻³), but high TP concentrations that ranged from 15 to 154 ng m⁻³ with an average TP concentration of 46 ng m⁻³, similar to spring. TP was not correlated with dust

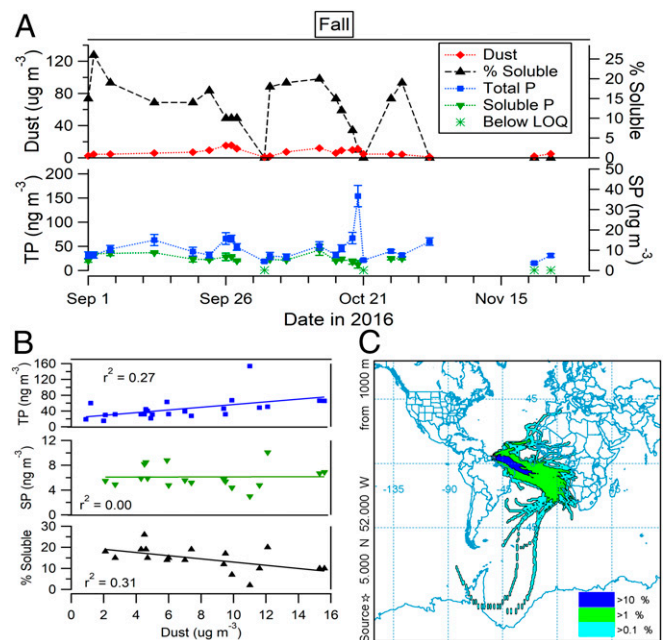


Fig. 2. Data are shown for fall only. *A* shows the dust concentration and percentage of SP in the *Top* and concentrations of TP and SP in the *Bottom*. Error bars for P measurements show one SD. *B* shows the correlation between TP and dust (*Top*), dust and SP (*Middle*), and percentage of soluble P and dust (*Bottom*). *C* shows HYSPLIT frequency plots of air mass back trajectories at 1,000 m initiated every 6 h from September 1 to October 31, 2016.

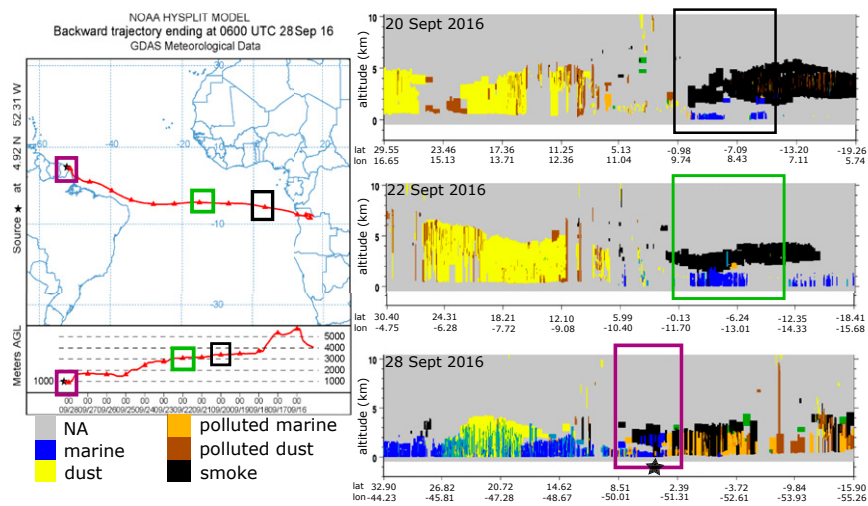


Fig. 3. A 315-h back trajectory initiated in Cayenne on September 28, 2016, at 1,000 m above ground level using HYSPLIT. *B–D* show the first 10 km of CALIPSO tracks that intersect the BT shown in *A* on (B) September 20, 2016, (C) September 22, 2016, and (D) September 28, 2016. The colored boxes in *A* correspond to the approximate location of where the CALIPSO overpass intersects the trajectory on September 20 (black box), September 22 (green box), and September 28 (purple box). Note that the altitude of the air mass is also boxed in corresponding colors. The black stars in *A* and *D* show the location of Cayenne.

during fall (Fig. 2 *B, Top*). Starting on August 1, PM_{10} was consistently greater than dust (SI Appendix, Fig. S2), suggesting that the aerosol mass in fall is dominated by sources other than dust. The low dust transport, presence of nondust aerosol, and lack of correlation between dust and TP suggest African dust is not the major source of P during fall. In fact, using a TP concentration of 1,080 ppm for dust, only 17% of TP can be explained by dust in fall. The SP concentrations in fall ranged from 3 to 10 $ng\ m^{-3}$ with an average concentration of 6 $ng\ m^{-3}$, the same average in spring. SP was not correlated with dust (Fig. 2 *B, Middle*), and the average P solubility in fall was 15%, which is twice as soluble as the P measured in spring. Furthermore, the solubility of P decreased as dust increased (Fig. 2 *B, Bottom*). These factors suggest that dust is not the main source of SP in fall.

There are several lines of evidence that suggest southern African BB is the source of P in fall. First, SEM images show BB aerosol on multiple collection days in September (SI Appendix, Fig. S7). Second, the filter color during fall was always gray (SI Appendix, Fig. S8), which is indicative of BC from BB. Third, air mass BT analysis showed that air masses originated from Africa south of the equator (Fig. 2C). Widespread BB in southern Africa occurs in boreal summer and fall (41) and can be transported across the Atlantic Ocean above the marine boundary layer (MBL) due to strong upper-level zonal winds from the southern African easterly jet (S-AEJ) (36, 42–46). Transport of this BB can occur as far north as 5°N, the latitude of Cayenne (28). Consistent with our findings, previous cruises in the Atlantic have measured increased TP and/or SP when air masses originated from southern Africa in fall (47–49).

To confirm that P measured in Cayenne in fall originated from southern African BB as opposed to Amazonian BB, which is also widespread in fall, we used the aerosol subtype product from the Cloud-Aerosol Lidar and Infrared Pathfinder Satellite Observation

(CALIPSO) and air mass BT analysis to investigate vertical profiles of BB across the Atlantic Ocean. Fig. 3A shows a representative 13-d air mass BT initialized on September 28, 2016 at 1,000 m. Fig. 3B–D show vertical profiles of aerosol types measured by CALIPSO, and the boxes shown in these figures indicate the location of the CALIPSO pass that intersects the air mass BT in Fig. 3A. Fig. 3B shows an elevated smoke plume (in black) observed close to Africa that is decoupled from the MBL and intersects the altitude of the BT. The CALIPSO pass in Fig. 3C also clearly shows an elevated smoke layer. The altitude of the smoke shown in the CALIPSO pass in Fig. 3C is corroborated by BC concentrations measured above the MBL on Ascension Island (50). Fig. 3D shows a CALIPSO pass close to Cayenne when the air mass BT was initiated. While the smoke layer originating from Africa has started to become entrained in the MBL, it clearly reaches Cayenne. Extended CALIPSO analysis in fall 2016 revealed that southern African BB is routinely transported across the Atlantic to Cayenne. Because P associated with BB is more soluble than P associated with dust (25, 48), our observations of higher P solubility in fall are best explained by southern African BB, which has also been shown to be transported to the interior of the Amazon (34, 35).

Smoke from southern Africa was detected in CALIPSO every day in fall when there were measurable quantities of SP in Cayenne. However, on days in October when SP was below the LOQ (SI Appendix, Fig. S9), smoke plumes were weaker, less distinct, and not observed over Cayenne (SI Appendix, Fig. S10). In November, SP was below the LOQ likely due to changes in air mass BT patterns (SI Appendix, Fig. S11) and a decrease in wind intensity of the S-AEJ (36) and fire activity in southern Africa. The simultaneous decrease of SP measured in Cayenne and southern African BB in November further supports our finding that southern African BB is the dominant source of SP in September and October.

Table 1. Annual average deposition of P (in teragrams per year) into the Amazon Basin associated with the long-range transport of African dust and BB

Study	P from African dust		P from African BB*	
	TP	SP	TP	SP
Yu et al., 2015 (8)	0.022	—	—	—
This study MERRA-2	0.011	0.0006	—	—
This study CAM	0.011–0.033	0.0006–0.002	0.0026–0.052	0.0004–0.008

For CAM, the lower estimate is from the untuned model, while the high values come from tuning the model to match the observations from this study

*Only from long-range transported African BB; excludes Amazonian BB sources.

Discussion and Implications

Estimates of P Deposition to the Amazon and Implications for Ecosystem Productivity. Observations made in Cayenne can be used to extrapolate P deposition from transported African aerosols to the Amazon Basin for two reasons: 1) air mass forward trajectory analysis shows easterly trade winds that pass over Cayenne typically continue into the interior of the Amazon (*SI Appendix, Fig. S12*), and 2) Cayenne only receives transported African aerosol and background sea spray aerosol (6). Therefore, observations from Cayenne provide key insights into the magnitude of African aerosol transported to the Amazon Basin downwind of Cayenne. We estimated P deposition to the Amazon from African dust and BB using two modeling approaches: The Modern-Era Retrospective Analysis for Research and Applications, Version 2 (MERRA-2) and the Community Atmosphere Model (CAM) (51), which has been previously used to provide P deposition estimates to the Amazon (3). We discuss both models and their caveats in *Materials and Methods* and *SI Appendix*. The MERRA-2 surface aerosol product has been shown to provide accurate dust estimates during dust events in the United States (52), Barbados (53, 54), and in this study in Cayenne (*SI Appendix, Fig. S13*). The MERRA-2 deposition product yielded a rate of $4 \text{ g m}^{-2} \text{ y}^{-1}$ for Cayenne, similar to dust input rates to the ocean measured in nearby sediment cores (55). MERRA-2 performed poorly for African BB due to the presence of BB emissions from within the Amazon, which are indistinguishable from African BB. Therefore, the CAM model was used to estimate P deposition from African BB and dust using simulations that separate the sources of P from different aerosols (56). Both modeling approaches estimate annual TP deposition to the Amazon from dust to range from 0.011 to $0.033 \text{ Tg TP y}^{-1}$ (Table 1). In comparison, analysis by Yu et al. (8) estimated a deposition of 0.006 – $0.037 \text{ Tg TP y}^{-1}$ from African dust, similar to our estimates. We provide an estimate of SP deposition from African dust to the Amazon (0.0006 – $0.002 \text{ Tg SP y}^{-1}$).

We also provide an estimated range for regional deposition of P to the Amazon from African BB in Table 1. To calculate the upper estimate, we tuned CAM to our P observations (*SI Appendix, Fig. S14*) by increasing dust by a factor of 2 and black carbon from BB by a factor of 60, which is similar to the factor used in Ward et al. (57). The lower estimate provided is not tuned to our observations but to observations in source regions (57, 58). CAM estimated the TP deposition from African BB to be up to $0.052 \text{ Tg TP y}^{-1}$ with SP accounting for up to $0.008 \text{ Tg SP y}^{-1}$ (Table 1), suggesting that African BB contributes up to the same amount of TP to the Amazon as dust. Fig. 4 uses the tuned CAM model to compare the fraction of TP (Fig. 4A) and SP (Fig. 4B) regionally deposited to the Amazon from African dust and both northern and southern African BB for each month in a year; BB emissions from within the Amazon were excluded. Fig. 4B shows that African BB contributes the majority of SP to the Amazon throughout the year, except in May, when BB emissions from the Sahel and fire activity in southern Africa are both low (41). Although TP deposition is dominated by dust from March to July, African BB is a considerable source of TP even when dust is high likely due to fire activity in the Sahel (41). In fall, southern African BB deposits nearly all of the TP and SP to the Amazon.

We estimate that African dust contributes between 11 and $35 \text{ g TP ha}^{-1} \text{ y}^{-1}$ while African BB supplies up to $55 \text{ g TP ha}^{-1} \text{ y}^{-1}$ to the Amazon. Previous studies of Amazon soil nutrient balance suggest that 8 to $40 \text{ g TP ha}^{-1} \text{ y}^{-1}$ are leached from the soil by rain (7). Thus, our estimated deposition rates—and potentially African BB deposition rates alone—could compensate such losses. Biogeochemical models currently consider all BB emissions to result in a net loss of P from the Amazon (3, 23), but our work shows that African BB emissions constitute a net influx of P. Biogeochemical models should account for seasonal P inputs from African BB to understand the net effect of BB on P budgets in the Amazon.

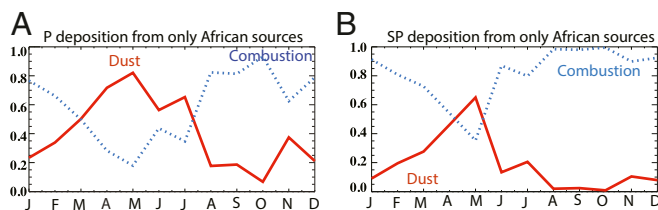


Fig. 4. Model predictions from CAM to estimate P deposition to the Amazon that were tuned to the observations to estimate the fraction of (A) TP deposition and (B) SP deposition from African dust (solid red line) and BB from both northern and southern Africa (dotted blue line). African dust and combustion sources of P are only included to investigate the relative importance of each transported source.

SP Deposition to the Ocean and Implications for Global Marine Primary Production. Primary production in the Atlantic Ocean is thought to be nitrogen (N) limited in low latitudes (10, 59). N can be supplied by N-fixing diazotrophs that require a supply of SP and soluble Fe to produce bioavailable N (10). Dust has been assumed to be the dominant source of these nutrients to the TAO year round (10, 15); however, the impact of dust on marine productivity is debated. In fact, a recent study (19) showed that dust has to be extensively acidified to supply SP to seawater, suggesting that other aerosol sources may be more important for providing soluble nutrients.

To investigate whether BB could be a more important supply of SP than dust, we used the CAM model to estimate global SP deposition from all aerosol sources (Fig. 5) and the SP contribution from BB and combustion alone (Fig. 6). Because SP deposition on a global scale was estimated as opposed to a regional scale, we included the global inventory of combustion and BB sources (including BB from the Amazon) (57, 60, 61), and we did not tune the model to our South American observations.

Fig. 5 shows CAM model estimates of global SP deposition from all aerosol sources. We estimate a deposition rate of between 0.1 and $1.0 \text{ mg SP m}^{-2} \text{ y}^{-1}$ over the TAO. The percent contribution of SP from BB and combustion alone to the global oceans was further investigated for each season (Fig. 6). BB accounts for 20% to 60% of SP deposition to the TAO in the summer (June–August; JJA) and fall (September–November; SON) and can be transported as far north as $\sim 5^\circ\text{N}$, consistent with the northward seasonal migration of the ITCZ (28, 62) and shipboard observations (18, 63). In summer, the influence of African BB is clear from Fig. 6; however, we note that the influence of BB on the TAO is a little less clear in fall from this modeling approach likely due to the strong signal from Amazonian BB and because CAM was not tuned to our observations. Our work also suggests that cotransported African BB from the Sahel may be an important source of SP during dust season in spring. Indeed, Fig. 6 shows a small protrusion of SP deposition from BB in spring (March–May; MAM) off the western coast of Africa, which is likely combustion in the Sahel.

Figs. 5 and 6 also extend estimates of SP deposition to the global oceans. Fig. 5 shows year-round SP deposition to the Indian and Southern Oceans of up to $0.5 \text{ mg SP m}^{-2} \text{ y}^{-1}$ from southern Africa, which Fig. 6 clearly shows is due to combustion and BB. Notably, because we did not tune CAM to our observations, the importance of BB and combustion for SP deposition to the oceans is likely underestimated and is more important than Fig. 6 suggests. Even without tuning CAM to our observations, our results suggest that African BB is more important than dust for alleviating P limitations in parts of the TAO, Indian Ocean, and Southern Ocean particularly in the summer and fall.

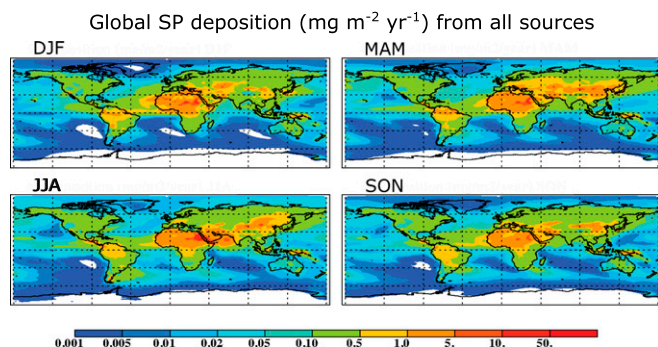


Fig. 5. SP deposition (in milligrams per square meter per year) from all aerosol sources during boreal winter (DJF), spring (MAM), summer (JJA), and fall (SON). Model predictions in this figure were not tuned to our observations.

Conclusions

We show that while African dust supplies the majority of the TP to the Amazon and TAO in spring, the P in dust is poorly soluble even after undergoing transport, which suggests that atmospheric processing played a limited role in increasing P solubility. Our results show that African BB supplies up to the same magnitude of TP to the Amazon as dust and is the dominant source of SP supplied to the Amazon. We further show that BB and combustion play a larger role than dust in the deposition of SP to the TAO, Indian Ocean, and Southern Ocean in summer and fall. Because BB emissions also contain soluble Fe (56, 64, 65), southern African BB likely has major implications for primary production in these ocean basins.

Climate change will likely affect the magnitude of aerosol deposition that relieves P-limitations (2, 9). While climate change is expected to influence African dust transport by a number of factors including precipitation, land use changes, and wind intensity (66–68), BB sources are more complicated. Industrial combustion emissions will likely increase due to an increasing human population, especially in Africa (25, 69). In the Sahel, land use conversion from frequently burned savanna to agricultural land is suppressing wildfire (70). In southern Africa wildfires are very sensitive to precipitation in the previous year (71). This work shows that changes in BB will strongly impact SP deposition to the Amazon, the TAO, and oceans in the Southern Hemisphere, with feedbacks on primary production and the drawdown of atmospheric carbon dioxide. Biogeochemical models should include current estimates of African BB and account for future changes in BB when predicting how primary production and the global carbon cycle will be affected by climate change. Finally, it should be noted that few aerosol measurements exist in South America. More extensive measurements across South America are needed to fully quantify our conclusions and to track changes in aerosol deposition over time.

Materials and Methods

Sample Collection, Dust Mass Quantification. Aerosols were collected on Whatman 41 cellulose filters using a high-volume sampler. Dust was measured using the method of Prospero et al. (72) by rinsing a portion of each filter with Milli-Q water to remove solubles, ashing samples to 500 °C, and quantifying the ash gravimetrically.

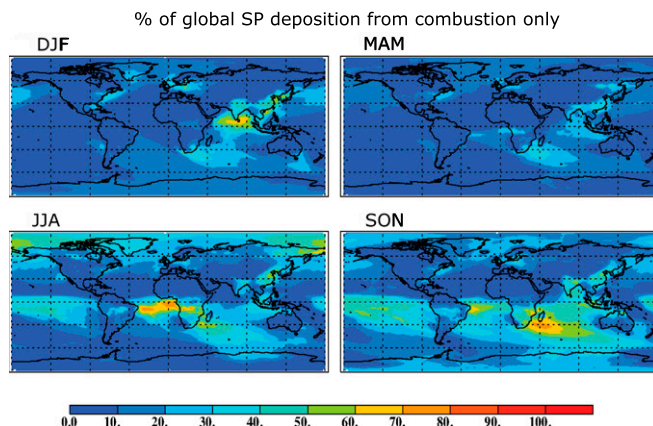


Fig. 6. Percentage of SP deposited from global BB sources only in boreal winter (DJF), spring (MAM), summer (JJA), and fall (SON). Model predictions in this figure were not tuned to our observations.

Air Mass Histories and Remote Sensing Products. Air mass back trajectories were computed using the Hybrid Single Particle Lagrangian Integrated Trajectory (HYSPPLIT) model (73, 74). Aerosol speciation products were obtained from the Cloud-Aerosol Lidar with Orthogonal Polarization (CALIOP) satellite using version 4.10.

Analysis of Total Phosphorus and Soluble Reactive Phosphorus (SRP). SRP (SP) was quantified by leaching a portion of an unwashed filter in a buffered (pH = 7) aqueous solution and using the colorimetric method (75, 76). TP was determined by ashing and acid digesting an unwashed filter portion followed by analysis on a Neptune Multicollector Inductively Coupled Plasma Mass Spectrometer.

Deposition Estimates. MERRA-2 was used to determine wet and dry dust deposition. CAM was used to estimate P deposition from dust and BB. For both modeling approaches, the deposition of TP and SP from dust was estimated using our values of 1,080 ppm of P in dust with a solubility of 5%. The deposition of TP and SP from BB was estimated with CAM using previously published P:BC ratios (3) and our value for P solubility of 15% as model input. The version of CAM used in this study was used to predict Fe deposition from different African sources, which were then converted to P using an Fe/BC ratio and the P and Fe content of dust. For the Amazon estimates shown in Table 1 and Fig. 4, CAM was forced to match the P observations at Cayenne by increasing dust by a factor of 2 and BC concentrations emitted by BB by 60-fold. We note that previously published work also increased BC concentrations manifold to match observations (57). This substantial enhancement in BC concentrations is likely due to a combination of factors including an underprediction of the BB inventory (57), higher P contributions from BB than predicted by currently used P:BC ratios, or inadequate transport from Africa in the model. For global estimates shown in Figs. 5 and 6, the global inventory of dust and BB was included, which was not tuned to our observations.

ACKNOWLEDGMENTS. We thank ATMO Guyane for collecting filter samples and maintaining the field site in Cayenne, French Guiana (<https://www.atmo-guyane.org/>). The authors acknowledge the National Oceanic and Atmospheric Administration (NOAA) Air Resources Laboratory (ARL) for the provision of the HYSPPLIT transport and dispersion model and READY website (<http://www.ready.noaa.gov>). We thank National Aeronautics and Space Administration (NASA) for making the CALIPSO and MERRA-2 data available to the scientific community. C.J.G. acknowledges funding provided by the Provost Award from the University of Miami. N.M. and D.S.H. acknowledge the support of the Atkinson Center for a Sustainable Future and the Department of Energy (DE-SC0006791). We thank anonymous reviewers for useful comments and suggestions.

1. R. Swap, M. Garstang, S. Greco, R. Talbot, P. Källberg, Saharan dust in the Amazon Basin. *Tellus* **44B**, 133–149 (1992).
2. N. Mahowald, Aerosol indirect effect on biogeochemical cycles and climate. *Science* **334**, 794–796 (2011).
3. N. M. Mahowald et al., Impacts of biomass burning emissions and land use change on Amazonian atmospheric phosphorus cycling and deposition. *Global Biogeochem. Cycles* **19**, GB4030 (2005).
4. G. S. Okin et al., Impacts of atmospheric nutrient deposition on marine productivity: Roles of nitrogen, phosphorus, and iron. *Global Biogeochem. Cycles* **25**, 1–10 (2011).

5. J. M. Prospero, R. A. Glaccum, R. T. Nees, Atmospheric transport of soil dust from Africa to South America. *Nature* **289**, 570–572 (1981).
6. J. M. Prospero, F. Collard, J. Molinié, A. Jeannot, Characterizing the annual cycle of African dust transport to the Caribbean Basin and South America and its impact on the environment and air quality. *Global Biogeochem. Cycles* **28**, 757–773 (2014).
7. P. M. Vitousek, R. L. Sandford, Nutrient cycling in moist tropical forest. *Annu. Rev. Ecol. Syst.* **17**, 137–167 (1986).
8. H. Yu et al., The fertilizing role of African dust in the Amazon rainforest: A first multiyear assessment based on CALIPSO lidar observations. *Geophys. Res. Lett.* **42**, 1984–1991 (2015).

9. G. S. Okin, N. Mahowald, O. A. Chadwick, P. Artaxo, Impact of desert dust on the biogeochemistry of phosphorus in terrestrial ecosystems. *Global Biogeochem. Cycles* **18**, GB2005 (2004).
10. M. M. Mills, C. Ridame, M. Davey, J. La Roche, R. J. Geider, Iron and phosphorus co-limit nitrogen fixation in the eastern tropical North Atlantic. *Nature* **429**, 292–294 (2004).
11. O. A. Chadwick, L. A. Derry, P. M. Vitousek, B. J. Huebert, L. O. Hedin, Changing sources of nutrients during four million years of ecosystem development. *Nature* **397**, 491–497 (1999).
12. Y. Ben-Ami *et al.*, Transport of North African dust from the Bodélé depression to the Amazon Basin: A case study. *Atmos. Chem. Phys.* **10**, 7533–7544 (2010).
13. C. S. Bristow, K. A. Hudson-Edwards, A. Chappell, Fertilizing the Amazon and equatorial Atlantic with West African dust. *Geophys. Res. Lett.* **37**, 3–7 (2010).
14. T. Jickells, C. M. Moore, The importance of atmospheric deposition for ocean productivity. *Annu. Rev. Ecol. Evol. Syst.* **46**, 481–501 (2015).
15. N. Mahowald *et al.*, Global distribution of atmospheric phosphorus sources, concentrations and deposition rates, and anthropogenic impacts. *Global Biogeochem. Cycles* **22**, 1–19 (2008).
16. K. A. Hudson-Edwards, C. S. Bristow, G. Cibir, G. Mason, C. L. Peacock, Solid-phase phosphorus speciation in Saharan Bodélé Depression dusts and source sediments. *Chem. Geol.* **384**, 16–26 (2014).
17. L. M. Zamora, J. M. Prospero, D. A. Hansell, J. M. Trapp, Atmospheric P deposition to the subtropical North Atlantic: Sources, properties, and relationship to N deposition. *J. Geophys. Res. Atmos.* **118**, 1546–1562 (2013).
18. A. R. Baker, T. D. Jickells, M. Witt, K. L. Linge, Trends in the solubility of iron, aluminium, manganese and phosphorus in aerosol collected over the Atlantic Ocean. *Mar. Chem.* **98**, 43–58 (2006).
19. L. F. Korte *et al.*, Effects of dry and wet Saharan dust deposition in the tropical North Atlantic Ocean. *Biogeosci. Discuss.* 1–20 (2018).
20. A. Nenes *et al.*, Atmospheric acidification of mineral aerosols: A source of bioavailable phosphorus for the oceans. *Atmos. Chem. Phys.* **11**, 6265–6272 (2011).
21. A. Stockdale *et al.*, Understanding the nature of atmospheric acid processing of mineral dusts in supplying bioavailable phosphorus to the oceans. *Proc. Natl. Acad. Sci. U.S.A.* **113**, 14639–14644 (2016).
22. A. R. Baker, M. French, K. L. Linge, Trends in aerosol nutrient solubility along a west-east transect of the Saharan dust plume. *Geophys. Res. Lett.* **33**, 10–13 (2006).
23. S. Myriokefalitakis, A. Nenes, A. R. Baker, N. Mihalopoulos, M. Kanakidou, Bioavailable atmospheric phosphorus supply to the global ocean: A 3-D global modeling study. *Biogeosciences* **13**, 6519–6543 (2016).
24. L. D. Anderson, K. L. Faul, A. Paytan, Phosphorus associations in aerosols: What can they tell us about P bioavailability? *Mar. Chem.* **120**, 44–56 (2010).
25. R. Wang *et al.*, Significant contribution of combustion-related emissions to the atmospheric phosphorus budget. *Nat. Geosci.* **8**, 48–54 (2015).
26. C. Textor *et al.*, Analysis and quantification of the diversities of aerosol life cycles within AeroCom. *Atmos. Chem. Phys.* **6**, 1777–1813 (2006).
27. M. Labonne, Injection height of biomass burning aerosols as seen from a spaceborne lidar. *Geophys. Res. Lett.* **34**, 1–5 (2007).
28. A. M. Adams, J. M. Prospero, C. Zhang, CALIPSO-derived three-dimensional structure of aerosol over the Atlantic basin and adjacent continents. *J. Clim.* **25**, 6862–6879 (2012).
29. C. I. Bovolo, R. Pereira, G. Parkin, C. Kilsby, T. Wagner, Fine-scale regional climate patterns in the Guianas, tropical South America, based on observations and reanalysis data. *Int. J. Climatol.* **32**, 1665–1689 (2012).
30. A. Ansmann *et al.*, Dust and smoke transport from Africa to South America: Lidar profiling over Cape Verde and the Amazon rainforest. *Geophys. Res. Lett.* **36**, 2–6 (2009).
31. C. Chou *et al.*, Size distribution, shape, and composition of mineral dust aerosols collected during the African Monsoon Multidisciplinary Analysis Special Observation Period 0: Dust and Biomass-Burning Experiment field campaign in Niger, January 2006. *J. Geophys. Res. Atmos.* **113**, 1–17 (2008).
32. T. Schneider, T. Bischoff, G. H. Haug, Migrations and dynamics of the intertropical convergence zone. *Nature* **513**, 45–53 (2014).
33. Y. Chen, “Sources and fate of atmospheric nutrients over the remote oceans and their role on controlling marine diazotrophic microorganisms,” PhD thesis, University of Maryland Center for Environmental Science, Cambridge, MD (2004).
34. J. Saturno *et al.*, Black and brown carbon over central Amazonia: Long-term aerosol measurements at the ATTO site. *Atmos. Chem. Phys.* **18**, 12817–12843 (2018).
35. D. Moran-Zuloaga *et al.*, Long-term study on coarse mode aerosols in the Amazon rain forest with the frequent intrusion of Saharan dust plumes. *Atmos. Chem. Phys.* **18**, 10055–10088 (2018).
36. A. A. Adebisi, P. Zuidema, The role of the southern African easterly jet in modifying the southeast Atlantic aerosol and cloud environments. *Q. J. R. Meteorol. Soc.* **142**, 1574–1589 (2016).
37. J. M. Prospero, O. L. Mayol-Bracero, Understanding the transport and impact of African dust on the Caribbean basin. *Bull. Am. Meteorol. Soc.* **94**, 1329–1337 (2013).
38. Y. J. Kaufman *et al.*, Dust transport and deposition observed from the Terra-Moderate Resolution Imaging Spectroradiometer (MODIS) spacecraft over the Atlantic Ocean. *J. Geophys. Res. Atmos.* **110**, 1–16 (2005).
39. P. Artaxo, H. Storms, F. Bruynseels, R. Van Grieken, W. Maenhaut, Composition and sources of aerosols from the Amazon Basin. *J. Geophys. Res.* **93**, 1605–1615 (1988).
40. G. Roberts, M. J. Wooster, E. Lagouidakis, Annual and diurnal African biomass burning temporal dynamics. *Biogeosciences* **6**, 849–866 (2009).
41. L. Giglio, J. T. Randerson, G. R. Van Der Werf, Analysis of daily, monthly, and annual burned area using the fourth-generation global fire emissions database (GFED4). *J. Geophys. Res. Biogeosci.* **118**, 317–328 (2013).
42. M. Garstang *et al.*, Horizontal and vertical transport of air over southern Africa. *J. Geophys. Res.* **101**, 23721–23736 (1996).
43. R. Swap *et al.*, The long-range transport of southern African aerosols to the tropical South Atlantic. *J. Geophys. Res. Atmos.* **101**, 23777–23791 (1996).
44. P. J. Crutzen, M. Andreae, Biomass burning in the tropics: Impact on atmospheric chemistry and biogeochemical cycles. *Science* **250**, 1669–1678 (1990).
45. W. F. Cooke, B. Koffi, J.-M. Grégoire, Seasonality of vegetation fires in Africa from remote sensing data and application to a global chemistry model. *J. Geophys. Res. Atmos.* **101**, 21051–21065 (1996).
46. S. Das *et al.*, Biomass burning aerosol transport and vertical distribution over the South African-Atlantic region. *J. Geophys. Res.* **122**, 6391–6415 (2017).
47. R. Losno, G. Bergametti, P. Carlier, Origins of atmospheric particulate matter over the North Sea and the Atlantic Ocean. *J. Atmos. Chem.* **15**, 333–352 (1992).
48. A. R. Baker, T. D. Jickells, K. F. Biswas, K. Weston, M. French, Nutrients in atmospheric aerosol particles along the Atlantic Meridional Transect. *Deep Res Part II Top Stud Oceanogr* **53**, 1706–1719 (2006).
49. C. F. Powell *et al.*, Estimation of the atmospheric flux of nutrients and trace metals to the eastern Tropical North Atlantic Ocean. *J. Atmos. Sci.* **72**, 4029–4045 (2015).
50. P. Zuidema *et al.*, The Ascension Island boundary layer in the remote southeast Atlantic is often smoky. *Geophys. Res. Lett.* **44**, 4456–4465 (2018).
51. R. A. Scanza *et al.*, Atmospheric processing of iron in mineral and combustion aerosols: Development of an intermediate-complexity mechanism suitable for Earth system models. *Atmos. Chem. Phys.* **18**, 14175–14196 (2018).
52. S. P. Chen, C. H. Lu, J. McQueen, P. Lee, Application of satellite observations in conjunction with aerosol reanalysis to characterize long-range transport of African and Asian dust on air quality in the contiguous U.S. *Atmos. Environ.* **187**, 174–195 (2018).
53. C. A. Randles *et al.*, The MERRA-2 aerosol reanalysis, 1980-onward, Part I: System description and data assimilation evaluation. *J. Clim.* **30**, 6823–6850 (2017).
54. V. Buchard *et al.*, The MERRA-2 aerosol reanalysis, 1980 onward. Part II: Evaluation and case studies. *J. Clim.* **30**, 6851–6872 (2017).
55. S. S. Kienast, G. Winkler, J. Lippold, S. Albani, N. M. Mahowald, Tracing dust input to the global ocean using thorium isotopes in marine sediments: ThoroMap. *Global Biogeochem. Cycles* **30**, 1526–1541 (2016).
56. N. M. Mahowald *et al.*, Aerosol trace metal leaching and impacts on marine microorganisms. *Nat. Commun.* **9**, 2614 (2018).
57. D. S. Ward *et al.*, The changing radiative forcing of fires: Global model estimates for past, present and future. *Atmos. Chem. Phys.* **12**, 10857–10886 (2012).
58. S. Albani *et al.*, Improved dust representation in the community atmosphere model. *J. Adv. Model. Earth Syst.* **6**, 541–570 (2014).
59. C. M. Moore *et al.*, Processes and patterns of oceanic nutrient limitations. *Nat. Geosci.* **6**, 701–710 (2013).
60. J. Brahney, N. Mahowald, D. S. Ward, A. P. Ballantyne, J. C. Neff, Is atmospheric phosphorus pollution altering global alpine lake stoichiometry? *Global Biogeochem. Cycles* **29**, 1369–1383 (2015).
61. C.-T. Chien *et al.*, Effects of African dust deposition on phytoplankton in the western tropical Atlantic Ocean off Barbados. *Global Biogeochem. Cycles* **30**, 716–734 (2016).
62. J. M. Trapp, F. J. Millero, J. M. Prospero, Trends in the solubility of iron in dust-dominated aerosols in the equatorial Atlantic trade winds: Importance of iron speciation and sources. *Geochem. Geophys. Geosyst.* **11**, 1–22 (2010).
63. A. R. Baker, T. Lesworth, C. Adams, T. D. Jickells, L. Ganzeveld, Estimation of atmospheric nutrient inputs to the Atlantic ocean from 50°N to 50°S based on large-scale field sampling: Fixed nitrogen and dry deposition of phosphorus. *Global Biogeochem. Cycles* **24**, 1–16 (2010).
64. H. Matsui *et al.*, Anthropogenic combustion iron as a complex climate forcer. *Nat. Commun.* **9**, 1593 (2018).
65. C. Luo *et al.*, Combustion iron distribution and deposition. *Global Biogeochem. Cycles* **22**, 1–17 (2008).
66. A. T. Evan, C. Flamant, S. Fiedler, O. Doherty, An analysis of aeolian dust in climate models. *Geophys. Res. Lett.* **41**, 5996–6001 (2014).
67. D. A. Ridley, C. L. Heald, J. M. Prospero, What controls the recent changes in African mineral dust aerosol across the Atlantic? *Atmos. Chem. Phys.* **14**, 5735–5747 (2014).
68. P. Ginoux, J. M. Prospero, T. E. Gill, N. C. Hsu, M. Zhao, Global-scale attribution of anthropogenic and natural dust sources and their emission rates based on MODIS deep blue aerosol products. *Rev. Geophys.* **50**, 1–36 (2012).
69. C. Lioussé, E. Assamoi, P. Criqui, C. Granier, R. Rosset, Explosive growth in African combustion emissions from 2005 to 2030. *Environ. Res. Lett.* **9**, 035003 (2014).
70. N. Andela *et al.*, A human-driven decline in global burned area. *Science* **356**, 1356–1362 (2017).
71. S. Archibald, D. P. Roy, B. W. van Wilgen, R. J. Scholes, What limits fire? An examination of drivers of burnt area in Southern Africa. *Glob. Change Biol.* **15**, 613–630 (2009).
72. J. M. Prospero, Long-term measurements of the transport of African mineral dust to the southeastern United States: Implications for regional air quality. *J. Geophys. Res.* **104**, 15917–15927 (1999).
73. A. F. Stein *et al.*, NOAA’s HYSPLIT atmospheric transport and dispersion modeling system. *Bull. Am. Meteorol. Soc.* **96**, 2059–2077 (2015).
74. G. Rolph, A. Stein, B. Stunder, Real-time Environmental Applications and Display system: READY. *Environ. Model. Softw.* **95**, 210–228 (2017).
75. J. D. H. Strickland, T. R. Parsons, *A Practical Handbook of Seawater Analysis* (Fisheries Research Bureau of Canada, 1972), 10.1002/iroh.19700550118.
76. D. L. Johnson, Simultaneous determination of arsenate and phosphate in natural waters. *Environ. Sci. Technol.* **5**, 411–414 (1971).